Introduction to Synthetic Aperture Radar (SAR) and SAR Interferometry

Margaret Cheney

Abstract. This paper presents a tutorial on the foundations of Synthetic Aperture Radar. The paper shows how a simple antenna model can be used together with a linearized scattering approximation to predict the received signal. The paper then outlines the conventional image formation process and shows how two images from different flight passes can be used to obtain topographic information.

§1. Introduction and Relation to Approximation Theory

Approximation theory can be thought of as the reconstruction of a function from incomplete information. This description applies to many inverse problems and imaging problems, in which one generally wants to determine properties of an object from remote measurements. A good example is Synthetic Aperture Radar (SAR) imaging, a very successful imaging technique that has been developed in the engineering community and which has received little attention from mathematicians.

In conventional strip-mode SAR imaging, a plane or satellite carrying an antenna flies along a straight track, which we will assume is in the direction of the x_2 axis. The antenna emits pulses of electromagnetic radiation in a directed beam perpendicular to the flight track (i.e., in the x_1 direction). These waves scatter off the terrain, and the scattered waves are detected with the same antenna. The received signals are then used to produce an image of the terrain. (See Figure 1.)

The data depend on two variables, namely time and position along the x_2 axis, so we expect to be able to reconstruct a function of two variables.

Approximation Theory X: Wavelets, Splines, and Applications
Charles K. Chui, Larry L. Schumaker, and Joachim Stöckler (eds.), pp. 167–177.

ISBN 0-8265-1416-2.

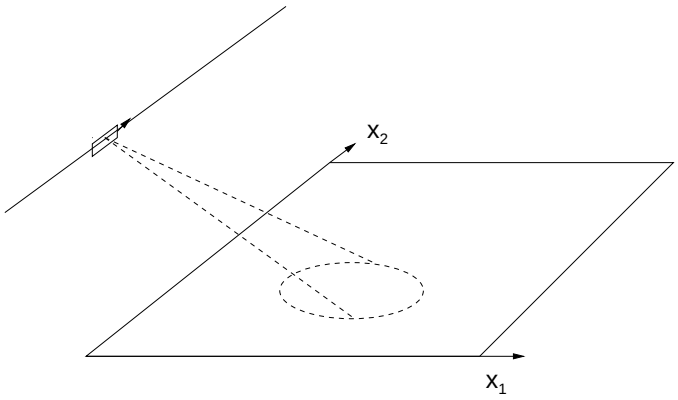

Fig. 1. Geometry of a SAR system.

§2. The Mathematical Model

A model for the wave propagation

The correct model for radar is of course Maxwell's equations, but the simpler scalar wave equation is commonly used:

$$\left(\nabla^2 - \frac{1}{c^2(x)}\partial_t^2\right) U(t,x) = 0. \tag{1}$$

This is the equation satisfied by each component of the electric and magnetic fields in free space, and is thus a good model for the wave propagation in dry air. When the electromagnetic waves interact with the ground, their polarization is certainly affected, but if the SAR system does not measure this polarization, then (1) is an adequate model.

We assume that the earth is roughly situated at the plane $x_3 = 0$, and that for $x_3 > 0$, the wave speed is $c(x) = c_0$, the speed of light in vacuum (a good approximation for dry air).

A model for the field from an antenna

In free space, the field $G_0(t,x)$ at x,t due to a delta function point source at the origin at time zero is given [15] by

$$G_0(t,x) = \frac{\delta(t-|x|/c_0)}{4\pi|x|}, \tag{2}$$

and satisfies the equation

$$\left(\nabla^2 - c_0^{-2}\partial_t^2\right) G_0(t,x) = -\delta(t)\delta(x). \tag{3}$$

The antenna, however, is not a point source $\delta(x)$; typical SAR satellite antennas are rectangular arrays measuring roughly 10m by 1m. Moreover, the delta function $\delta(t)$ on the right side of (3) is not a good model for the signal sent to the antenna; typically a *chirp* of the form $P(t) = \exp(i\alpha t^2)$ (over a limited time interval) is used. The field U^{in} emanating from the antenna then satisfies an equation of the form (3) with $\delta(t)$ replaced by the waveform $P(t)$, and $\delta(x)$ replaced by the current distribution $J(x)$ over the antenna.

The field emanating from the antenna then satisfies

$$\left(\nabla^2 - c_0^{-2}\partial_t^2\right) U^{in}(t,x) = -P(t)J_s(x), \tag{4}$$

so that

$$U^{in}(t,x) = G_0 * (PJ) = \int \frac{P(t-|x-y|/c_0)}{4\pi|x-y|} J(y)dy, \tag{5}$$

where the star denotes convolution in t and x.

We write P in terms of its Fourier transform $\tilde{P}$:

$$P(t) = \int e^{-i\omega t}\tilde{P}(\omega)d\omega. \tag{6}$$

In all SAR systems, $\tilde{P}(\omega)$ is negligible outside an interval which we call the frequency band. An important special case arises when the effective support is a narrow band (i.e., interval) centered at the carrier frequency ω_0; in this case it is useful to write

$$P(t) = A(t)e^{i\omega_0 t}, \tag{7}$$

where A is a slowly varying amplitude that is allowed to be complex. All the present satellite systems are narrowband systems for which (7) is most useful, but some of the airborne systems are broadband systems for which (7) is inappropriate and (6) is more useful. Using (6) in (5) gives us

$$U^{in}(t,x) = \int\int \frac{e^{-i\omega(t-|x-y|/c_0)}}{4\pi|x-y|}\tilde{P}(\omega)d\omega J(y)dy. \tag{8}$$

Next we assume that the antenna is small compared with the distance from the antenna to the ground. We denote the center of the antenna by y^0; thus a point on the antenna can be written $y = y^0 + q$, where q is a vector from the center of the antenna to a point on the antenna. In this notation, the assumption that the scattering point x is far from the antenna can be expressed $|q| << |x - y^0|$. For such x, we can write

$$|x-y| = |x-y^0| - (\widehat{x-y^0})\cdot q + O(q^2/|x-y^0|), \tag{9}$$

where the hat denotes a unit vector. We use the expansion (9) in (8) to obtain

$$\begin{aligned} U^{in}(t,x) &\approx \int\int \frac{e^{-i\omega(t-|x-y^0|)}}{4\pi|x-y^0|} e^{-i\omega(\widehat{x-y^0})\cdot q} \tilde{P}(\omega) d\omega J(y^0+q) dq \\ &\approx \int \frac{e^{-i\omega(t-|x-y^0|)}}{4\pi|x-y^0|} \tilde{P}(\omega) \tilde{J}(\omega, x, y^0) d\omega, \end{aligned} \tag{10}$$

where we have written

$$\tilde{J}(\omega, x, y^0) = \int e^{-i\omega(\widehat{x-y^0})\cdot q} J(y^0+q) dq.$$

This Fourier transform of the current density gives the antenna beam pattern in the far-field at each fixed frequency. A typical example is the case in which J is constant over a rectangular antenna. The antenna beam pattern $\tilde{J}$ is then a product of sinc functions, so that the antenna directs a beam perpendicular to the face of the antenna. At a frequency ω, the width of this beam is roughly $2\lambda/L$, where $\lambda = c_0/(2\pi\omega)$ is the wavelength and L is the length of the antenna.

Generally, the antenna beam pattern is nearly independent of frequency over the frequency band of $\tilde{P}(\omega)$; indeed, a great deal of work goes into designing antennas for which this is the case. Antennas whose beam patterns are nearly constant over a wide frequency band are called broadband antennas. For such antennas, (10) becomes

$$U^{in}(t,x) \approx \frac{P(t-|x-y^0|)}{4\pi|x-y^0|} \tilde{J}(\omega_0, x, y^0).$$

A linearized scattering model

Since we are ignoring polarization effects, the current density J is scalar and the model we use for wave propagation, including the source, is

$$\left(\nabla^2 - c_0^{-2}\partial_t^2\right) U(t,x) = -P(t) J_s(x). \tag{11}$$

We write $U = U^{in} + U^{sc}$ in (11) and use (4) to obtain

$$\left(\nabla^2 - c_0^{-2}\partial_t^2\right) U^{sc}(t,x) = -V(x)\partial_t^2 U(t,x), \tag{12}$$

where

$$V(x) = \frac{1}{c_0^2} - \frac{1}{c^2(x)}.$$

Most SAR systems operate at frequencies for which the waves do not penetrate appreciably into the earth. Thus we can approximate V by

$V(x) = V(x')\delta(x_3)$, where $x' = (x_1, x_2)$. We can write (12) as an integral equation

$$U^{sc}(t,x) = \int\int G_0(t-\tau, x-z)V(z)\partial_\tau^2 U(\tau,z)d\tau dz. \tag{13}$$

The single-scattering or Born approximation is to replace the full field U on the right side of (13) by the incident field U^{in}:

$$U^{sc}(t,x) \approx \int\int G_0(t-\tau, x-z)V(z)\partial_\tau^2 U^{in}(\tau,z)d\tau dz. \tag{14}$$

The value of this approximation is that it *linearizes* the inverse problem: the product of unknowns VU is replaced by the product of the unknown V with the known incident field.

With (2) and the expression (10) for the incident field from an antenna at position y^0, (14) becomes

$$\begin{aligned} U^{sc}_{y^0}(t,x) &\approx \int\int \frac{\delta(t-\tau-|x-z|/c_0)}{4\pi|x-z|}V(z) \\ &\quad \cdot \int \frac{e^{-i\omega(\tau-|z-y^0|/c_0)}}{4\pi|z-y^0|}\tilde{P}(\omega)\tilde{J}(\omega,z,y^0)\omega^2 d\omega d\tau dz \\ &\approx \int\int \frac{e^{-i\omega((t-(|x-z|+|z-y^0|)/c_0)}}{(4\pi)^2|x-z||z-y^0|}\tilde{P}(\omega)\tilde{J}(\omega,z,y^0)\omega^2 d\omega\ V(z)dz. \end{aligned}$$

At the center of the antenna,

$$U^{sc}_{y^0}(t,y^0) \approx \int\int \frac{e^{-i\omega(t-2|z-y^0|/c_0)}}{(4\pi)^2|z-y^0|^2}\tilde{P}(\omega)\tilde{J}(\omega,z,y^0)\omega^2 d\omega\ V(z)dz.$$

In practice, measurements are not simply made at the center of the antenna; instead what is measured is the integral of the field over the whole antenna. This gives rise to another antenna pattern which, in most cases, is the same as the transmission antenna beam pattern. In this case, the expression for the signal measured at antenna location y is

$$S(t,y) = U^{sc}_y(t,y) \approx \int\int \frac{e^{-i\omega(t-2|z-y|/c_0)}}{(4\pi)^2|z-y|^2}\tilde{P}(\omega)\tilde{J}^2(\omega,z,y)\omega^2 d\omega\ V(z)dz. \tag{15}$$

For a narrowband system, we have

$$S_N(t,y) \approx \int \frac{P(t-2|z-y|/c_0)}{(4\pi)^2|z-y|^2}\tilde{J}^2(\omega_0,z,y)\omega_0^2\ V(z)dz. \tag{16}$$

In (15) we are implicitly making the *start-stop* approximation, i.e., we are assuming that the antenna is stationary while it is transmitting and receiving. This is a good approximation because the antenna speed is so much slower than the speed of propagation of the electromagnetic signals.

From knowledge of the signal S for a large interval in t and for y along a line, we want to determine V.

§3. Formation of the Image

The idea underlying SAR reconstruction algorithms is to apply a matched filter to the measured signal (15). Applying a matched filter means integrating the signal against a shifted copy of the complex conjugate of the transmitted signal:

$$I(x) = \int\int \overline{P(t-2|x-y|/c_0)} S(t,y)\,dt\,dy. \tag{17}$$

For a narrowband system, the term matched filter is a natural one: taking $V(z) = \delta(z-x)$ in (16) shows that the measured signal from a point scatterer at position x is proportional to $P(t-2|x-y|/c_0)$. Thus in (17) we are "matching" the received signal to the signal that would have been received from a point scatterer at x. The "matching" process is done by taking the inner product; we expect that the integral (17) will be a maximum when the signal $S(t,y)$ is proportional to $P(t-2|x-y|/c_0)$. Under certain hypotheses on the noise, it is known that a matched filter gives the optimal signal-to-noise ratio in the class of linear filters [3,12].

The matched filter operation (17) is also called backprojection because it corresponds to summing all the signals to which a scatterer at x could have contributed. This amounts to summing over all spheres passing through the point x. Summing over the antenna locations y corresponds to forming a synthetic aperture, and, roughly speaking, corresponds to synthesizing the data one would have obtained from an extremely long antenna. Using (15) in (17) results in

$$\begin{aligned} I(x) &\approx \int\int \overline{P(t-2|x-y|/c_0)} \\ &\qquad \cdot \int\int \frac{e^{-i\omega(t-2|z-y|/c_0)}}{(4\pi)^2|z-y|^2} \tilde{P}(\omega)\tilde{J}^2(\omega,z,y)\omega^2 d\omega\; V(z)\,dz\,dt\,dy \\ &\approx \int\int\int \frac{e^{-i\omega(2(|x-y|-|z-y|)/c_0)}}{(4\pi|z-y|)^2} |\tilde{P}(\omega)|^2 \tilde{J}^2(\omega,z,y)\omega^2 d\omega\,dy\; V(z)\,dz. \end{aligned} \tag{18}$$

The last equation of (18) can be written as

$$I(x) = \int W(x,z)V(z)\,dz,$$

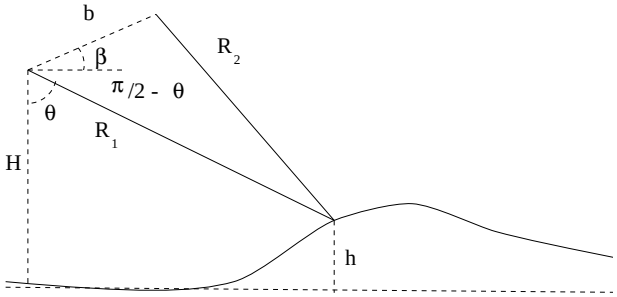

Fig. 2. Geometry for stereometry.

where

$$W(x,z) = \int\int \frac{e^{-i\omega(2(|x-y|-|z-y|)/c_0)}}{(4\pi|z-y|)^2} |\tilde{P}(\omega)|^2 \tilde{J}^2(\omega(\widehat{z-y}))\omega^2 d\omega dy$$

is the point spread function of the imaging system. This term arises because $W(x,z)$ is the image that would result from a point scatterer (i.e., delta function) located at the point z.

We see from a large-ω stationary phase analysis of W that the main contribution to W does indeed arise from the point $x = z$. An analysis of the resolution, which can be found in many references (for example [2,4,17]), shows that resolution in the range (i.e., distance from the antenna track) is determined by the bandwidth of the signal. The resolution in the along-track direction is determined by the effective aperture, which is the distance the antenna travels while keeping a given point in the beam. For narrowband systems, it turns out that the along-track resolution is independent of range and wavelength, and is better for small antennas.

§4. Determination of Ground Topography

In this section, instead of assuming the earth is flat, we assume that it has a varying elevation h, which we want to determine. In other words, we take the ground reflectivity function V to be of the form $V(z) = V(z')\delta(z_3 - h(z'))$, where $z' = (z_1, z_2)$.

If two images are made from two separate, known flight tracks, then in principle the elevation of an object that appears in both images can be determined by stereometry [8].

Stereometry

Suppose the first flight track is flown at height H, and the second is flown a distance b and angle of elevation β from the first. If the same object can be identified in both images, then its distances (ranges) R_1 and R_2 from the first and second flight track, respectively, can be determined. (See Figure 2.)

From R_1, R_2, b, and β, we can determine the angle of elevation θ from the law of cosines:

$$\begin{aligned} R_2^2 &= R_1^2 + b^2 - 2bR_1\cos(\beta + \frac{\pi}{2} - \theta) \\ &= R_1^2 + b^2 + 2bR_1\sin(\theta - \beta), \end{aligned} \tag{19}$$

and from knowledge of θ, the object's elevation h can be determined from $h = H - R_1\cos\theta$.

The difficulty with this method is twofold. First, it requires that common objects be identified in both images; this often requires human intervention. Second, the process is very sensitive to errors in the determination of the range difference $\Delta R = R_2 - R_1$. To see this, we use the chain rule

$$\frac{dh}{d(\Delta R)} = \frac{dh}{d\theta}\frac{d\theta}{d(\Delta R)} = R_1\sin\theta\frac{d\theta}{d(\Delta R)} \tag{20}$$

and calculate the derivative $d\theta/d(\Delta R)$ implicitly from (19) with $R_2 = R_1 + \Delta R$:

$$\frac{d\theta}{d(\Delta R)} = -\frac{R_1 + \Delta R}{bR_1\cos(\theta - \beta)}.$$

Using this in (20) gives

$$\frac{dh}{d(\Delta R)} = \frac{-(R_1 + \Delta R)\sin\theta}{b\cos(\theta - \beta)} \approx \frac{-R_2}{b}. \tag{21}$$

For satellite-borne SAR systems, the ratio R_2/b is very large; for the ERS-1 SAR, for example, R_1 and R_2 are both on the order of 800 km, and the baseline b is about 100 m [8]. Thus in estimating the ground height, range errors are magnified by a factor of 8000; the range resolution ΔR, however, is about 10 m, which means that the uncertainty in the estimated height is about 8 km, which is clearly unacceptable. It is for this reason that many SAR systems use instead an interferometric method to estimate ΔR and thus find the ground topography.

Interferometry

The interferometric technique applies to narrow-band SAR systems, for which (16) applies. Using (7) in (16) results in

$$S_N(t,y) \approx \int \frac{e^{-i\omega_0(t-2|z-y|/c_0)}}{(4\pi)^2|z-y|^2} A(t - 2|z-y|/c_0)\tilde{J}^2(\omega_0(\widehat{z-y}))\omega_0^2 V(z)dz. \tag{22}$$

The reflectivity function V we assume to be of the form $V(z) = V(z_T)$ $\delta(z_3 - h(z_T))$ where we have written $z_T = (z', 0)$ and $z = z_T + h\hat{e}_3$. (See

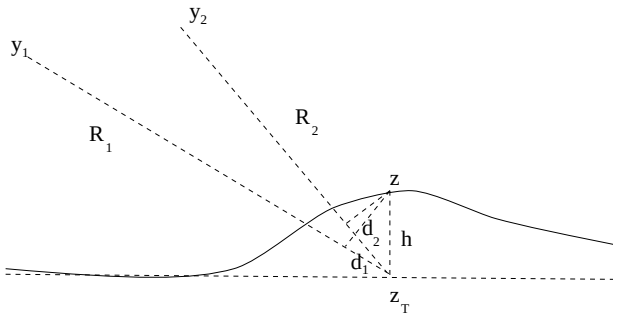

Fig. 3. Geometry for interferometry.

Figure 3.) We assume also that the height h is much less than the distance from the antenna to the ground, so that

$$|z-y| = |z_T + h\hat{e}_3 - y| = |z_T - y| - \widehat{z_T - y} \cdot h\hat{e}_3 + O(h^2/|z_T - y|). \quad (23)$$

We use this expansion in the expression (22) for the received signal, obtaining

$$S_N(t,y) \approx \int \frac{e^{-i\omega_0(t-2|z_T-y|/c_0)}}{(4\pi)^2|z_T-y|^2} A(t-2|z_T-y|/c_0)\omega_0^2 \cdot \tilde{J}^2(\omega_0(\widehat{z_T-y}))e^{2i\omega_0 d(z_T)/c_0} V(z_T)dz_T,$$

where we have written $d(z_T) = \widehat{z_T - y} \cdot h\hat{e}_3$ and where we have used the fact that A is slowly varying. We see that S_N corresponds to the signal that would have been obtained from a flat earth with complex reflectivity function $e^{2i\omega_0 d(z_T)/c_0}V(z_T)$. The image formation process of Section 3 will thus result in a complex-valued image, in which the phase at each point contains information about the height of the ground at that point.

This information is extracted as follows. Two separate, known flight tracks are each used to produce a complex-valued image, in which the pixel at location z_T represents the quantity $e^{2i\omega_0 d(z_T)/c_0}V(z_T)$. In the jth image, this pixel occurs at range $r_j = |y_j - z_T|$; the true range is $R_j = r_j - d_j \approx |y_j - z|$. The two images are *co-registered* to make $r_1 = r_2$. The complex conjugate of one image is then multiplied by the other, resulting in a complex image whose phase at z_T is $2\omega_0(d_1(z_T) - d_2(z_T))/c_0$; from this, the range difference $d_1 - d_2$ is found (after solving a phase unwrapping problem). Then (19) can be used with $R_2 = R_1 + (d_1 - d_2)$.

The determination of $\Delta R = d_1 - d_2$ can be done with great accuracy; for example, to millimeter accuracy in the case of the ERS-1 satellite [8]. The estimate (21) then results in an uncertainty in h of the order of meters.

Acknowledgments. This work was partially supported by the National Science Foundation Engineering Research Centers Program under award number EEC-9986821 and by the Focus Groups in Mathematical Sciences Program.

References

1. Bamler, R. and P. Hartl, Synthetic aperture radar interferometry, Inverse Problems **14** (1998), R1–R54.
2. Cheney, M., A mathematical tutorial on Synthetic Aperture Radar, SIAM Review **43** (2001), 301–312.
3. Curlander, J. C. and R. N. McDonough, *Synthetic Aperture Radar*, Wiley, New York, 1991.
4. Cutrona, L. J., Synthetic Aperture Radar, in *Radar Handbook*, second edition, ed. M. Skolnik, McGraw-Hill, New York, 1990.
5. Edde, B., *Radar: Principles, Technology, Applications*, Prentice Hall, New York, 1993.
6. Elachi, C., *Spaceborne Radar Remote Sensing: Applications and Techniques*, IEEE Press, New York, 1987.
7. Guyenne, T.-D., ed., *Engineering Achievements of ERS-1*, European Space Agency SP-1197/III, ESA Publications Division, ESTEC, Noordwij, The Netherlands, 1977.
8. Franceschetti, G. and R. Lanari, *Synthetic Aperture Radar Processing*, CRC Press, New York, 1999.
9. Langenberg, K. J, M. Brandfass, K. Mayer, T. Kreutter, A. Brüll, P. Felinger, D. Huo, Principles of microwave imaging and inverse scattering, EARSeL Advances in Remote Sensing, **2** (1993), 163–186.
10. Langenberg, K. J., Applied inverse problems, in *Basic Methods of Tomography and Inverse Problems*, ed. P.C. Sabatier, Adam Hilger, Bristol, 1987.
11. Natterer, F., *The Mathematics of Computerized Tomography*, Wiley, New York, 1986.
12. North, D. O., An analysis of the factors which determine signal/noise discrimination in pulsed-carrier systems, Proc. IEEE **51** (1963), 1016–1027 (reprint of RCA Technical Report PTR-6C, June 25, 1943).
13. Oppenheim, A. V. and R. W. Shafer, *Digital Signal Processing*, Prentice-Hall, Englewood Cliffs, New Jersey, 1975.
14. Soumekh, M., *Synthetic Aperture Radar Signal Processing with MATLAB Algorithms*, Wiley, New York, 1999.
15. Treves, F., *Basic Linear Partial Differential Equations*, Academic Press, New York, 1975.

16. Therrien, C. W., *Discrete Random Signals and Statistical Signal Processing*, Prentice Hall, Englewood Cliffs, New Jersey, 1992.
17. Ulander, L. M. H., and H. Hellsten, A new formula for SAR spatial resolution, AEÜ Int. J. Electron. Commun. **50** (1996) no. 2, 117–121.
18. Ulander, L. M. H., and P.-O. Frölund, Ultra-wideband SAR interferometry, IEEE Trans. on Geoscience and Remote Sensing, **36** no. 5, September 1998, 1540–1550.
19. Ziomek, L. J., *Underwater Acoustics: A Linear Systems Theory Approach*, Academic Press, Orlando, 1985.

Margaret Cheney
Department of Mathematical Sciences
Rensselaer Polytechnic Institute
Troy, NY 12180 USA
cheney@rpi.edu
http://www.rpi.edu/∼cheney